Moroccan Journal of Chemistry
ISSN : 2351-812X

Mor. J. Chem., 2023, Volume 11, Issue 3, Page 854-870
https://revues.imist.ma/index.php/morjchem
https://doi.org/10.48317/IMIST.PRSM/morjchem-v11i3.40434

Modification of Nanozirconia with Sulfuric Acid and Calcium Oxide as Heterogeneous Catalysts for Biodiesel Production from Used Coconut Cooking Oil

A. I. Agipa [1], W. D. Saputri [2], A. Syoufian [1], S. Sudiono [1], A. Budiman [3], M. F. Lestari [4], L. Hauli [5], K. Wijaya [1*]

[1]*Department of Chemistry, Faculty of Mathematics and Natural Sciences, Universitas Gadjah Mada, Yogyakarta 55281, Indonesia*
[2]*Research Center for Quantum Physics, National Research and Innovation Agency (BRIN), South Tangerang 15314, Indonesia*
[3]*Department of Chemical Engineering, Faculty of Engineering, Universitas Gadjah Mada, Yogyakarta 55281, Indonesia*
[4]*Department of Chemical Analysis, Akademi Komunitas Industri Manufaktur Bantaeng, Bantaeng 92461, South Sulawesi, Indonesia*
[5]*Research Center for Chemistry, National Research and Innovation Agency (BRIN), South Tangerang 15314, Indonesia*
**Corresponding author, Email address: karnawijaya@ugm.ac.id*

Received *26 May 2023,*
Revised *07 July 2023,*
Accepted *09 July 2023*

Citation*: Agipa A. I., Saputri W. D., Syoufian A., Sudiono S., Budiman A., Lestari M. F., Hauli L., Wijaya K. (2023) Modification of Nanozirconia with Sulfuric Acid and Calcium Oxide as Heterogeneous Catalysts for Biodiesel Production from Used Coconut Cooking Oil, Mor. J. Chem., 14(3), 854-870.*

Abstract: The commercial zirconia nanopowder was modified using sulfuric acid and calcium oxide to synthesize SO_4/ZrO_2 and Zr/CaO catalysts. The wet impregnation technique was utilized to obtain SO_4/ZrO_2 acid catalyst, and the Zr/CaO base catalyst was produced as well using reflux method through the microwave heating process. The highest total acidity of SO_4/ZrO_2 catalyst was treated by 0.9 M H_2SO_4 and 500 °C of calcination temperature, and this catalyst was succeeded in reducing used coconut cooking oil FFA from 1.18% to 0.42% in the esterification process. The highest total alkalinity was reached using 1% w/w Zr/CaO and 900 °C of calcination temperature, and this catalyst was applied in the transesterification stage and successfully converted used coconut cooking oil into biodiesel by 62.25%. The formation of biodiesel was confirmed by the presence of methyl laurate (50.48%), methyl myristate (19.05%), methyl stearate (11.05%), methyl 11-octadecanoic (6.09%), methyl octanoate (5.25%), methyl decanoate (5.05%), and methyl octadecanoate (3.03%).

Keywords: SO_4/ZrO_2 catalyst, Zr/CaO catalyst, Biodiesel, Esterification, Transesterification.

1. Introduction

Biodiesel is a sustainable energy source developed from vegetable/Phyto oils and animal fats whose excellent properties, such as environmentally friendly, high boiling points, good lubrication capabilities, and suitable candidate as an alternative of fossil fuels (Ma *et al*., 1999; Usman B. & Dambazau (2018), Rosina *et al*., 2022). Canola, sunflower, Jatropha, rapeseed, coconut, and palm oil have been used as raw materials for producing biodiesel. From the various raw materials, coconut oil has very high potential because of its abundant availability (Fu *et al*., 2009; Aman *et al*., 2018). In the past several years, many researchers have produced biodiesel from inedible vegetable oils as raw

materials since edible oils can cause food security problems. Coconut cooking oil is the primary waste product of cooking activities in restaurants and homes, making it a valuable replacement for edible oil (Kumar *et al*., 2012; Niyas & Shaija 2023).

In the biodiesel-produced process, homogeneous base catalysts (e.g., NaOH, KOH, CaO, and NaOMe) (Kaur *et al*., 2013) or homogeneous acid catalysts (e.g., H_2SO_4 and HCl) (Cao *et al*., 2008) are used for the triglyceride reaction process with alcohol. The application of a homogeneous base catalyst is able to increase the rate of biodiesel formation reaction. On the other hand, it is more expensive because the biodiesel must be washed to remove the catalysts. Nowadays, a heterogeneous catalyst is widely applied for biodiesel production due to easily separated, reusable, and preventing product contamination as well. ZrO_2 is a metal oxide group that is frequently used in the production of heterogeneous catalysts because it has excellent thermal stability, low thermal conductivity, high resistance to corrosion, and the ability to be converted into acid or base catalysts with good ion exchange capacity and redox activity in the catalytic process (Yamaguchi, 1994; Wang *et al*., 2022; Mabate *et al*., 2023).).

Typically, biodiesel is usually produced by the transesterification reaction of oil or fat with alcohol. In oil with an FFA and water content of more than 0.5% and 0.3%, respectively, are going to form a saponification reaction due to a deactivation catalyst that causes reduced biodiesel production (Fu *et al*., 2009). The esterification reaction is necessary as a pretreatment to reduce the FFA level and water content thus the saponification reaction will not be formed. Nurhayati et al. (2017) have succeeded in making biodiesel with two reaction stages, the esterification with a sulfuric acid catalyst to reduce FFA levels in oil and transesterification with CaO catalyst capable of producing biodiesel from palm oil 87.17% (Nurhayati *et al*., 2017).

One of the catalysts often used in esterification reactions is sulfated zirconia (SO_4/ZrO_2). Zirconia is used as a carrier for its good stability and weak acid sites. The development of sulfate ions on zirconia surfaces is able to increase the total acidity of the catalyst (Saravanan *et al*., 2012). Dopped sulfate ions on the zirconia surface cause super heterogeneous acid catalyst formation because the sulfate ion is a complexing agent stronger than chloride or nitrate ions (Clearfield *et al*., 1994; Sekewael *et al*., 2022; Delarmelina *et al*., 2021).

Calcium oxide (CaO) is a heterogeneous base catalyst that promises to be used in biodiesel formation because its solubility is low, it is not susceptible to the reaction, and the separation between product and catalyst is highly convenient (Mahardika *et al*., 2017). In addition, CaO has a high basicity value, is non-corrosive, and is environmentally friendly (Zein *et al*., 2016). A researcher reported that CaO has covalent characters that can facilitate transesterification reactions and produce high biodiesel yields (Suprapto *et al*., 2016). However, CaO has a weak mechanical strength, which attends to the disruption of catalyst in a reactor and limits its application. Modifications of CaO with metal oxide can improve catalyst stability (Xia *et al*., 2014; Garba *et al*., 2021) and can be done by employing thermal decomposition, impregnation, mixing, and precipitation (Banković-Ilić *et al*., 2017). Kaur and Ali (2014) report have succeeded in obtaining Fatty Acid Methyl Ester (FAME) and Fatty Acid Ethyl Ester (FAEE) more than 99% through transesterification reaction of Jatropha curcas oil using Zr/CaO catalyst (Kaur and Ali, 2014). La Ore et al. (2020) also successfully synthesized 15% Zr/CaO catalysts via the hydrothermal method, then was used for the transesterification process for low grade coconut palm oil into biodiesel until 69.52%.

In this study, the synthesis method of Zr/CaO base catalyst through reflux with heating using microwaves. Hsiao et al. (2020) compared bromooctane modified CaO catalyst synthesized by microwave heating for 2 hours with conventional heating for 24 hours having the same catalyst

characteristics to obtain biodiesel from waste cooking oil. In addition, the energy consumed in the synthesis using microwaves is 2160 kJ, ten times lower than the synthesis using conventional heating (21600 kJ). To the best of our observation, there has been no investigation into the production of biodiesel from used coconut oil utilizing a Zr/CaO catalyst synthesized by microwave heating techniques.

This study utilized coconut cooking oil as a source material for biodiesel conversion. Esterification utilizing a heterogeneous acid catalyst of SO_4/ZrO_2 was followed by transesterification utilizing a heterogeneous base catalyst of Zr/CaO in the production of biodiesel.

2. Methodology

2.1 Materials

The materials handled in this study consisted of Used Coconut Cooking Oil (UCCO) from food merchant in Tamansiswa, Yogyakarta, commercial zirconia nanopowder (ZrO_2 60-70 nm) from JiaozouHuasu Chemical Co., Ltd (Henan, China), zirconium (IV) oxychloride octahydrate ($ZrOCl_2 \cdot 8H_2O$), CaO technical and H_2SO_4, HCl, NaOH, KOH, CH_3OH, Na_2SO_4, $C_2H_2O_4$ pro analysis from Merck.

2.2 Synthesis of SO_4/ZrO_2 acid catalyst

SO_4/ZrO_2 catalyst was synthesized via wet impregnation method. The 10 g of ZrO_2 was added to 150 mL H_2SO_4 with concentrations at 0.5; 0.7; and 0.9 M, then stirred. A temperature of 105 ℃ is selected to dry the sample and followed by calcination at 400, 500, 600, and 700 ℃. Adsorption of ammonia is utilized to establish the total acidity of the catalyst by the gravimetric methods.

2.3 Synthesis of Zr/CaO base catalyst

Zr/CaO catalyst was produced using the reflux method heated with the microwave. The weight variations of Zr on $ZrOCl_2 \cdot 8H_2O$ of 1, 3, and 5% against CaO were carried out. The mixture was refluxed at 80 ℃ then centrifuged. Samples were drained at 120 ℃ and calcined at 600, 700, 800, and 900 ℃. The acidity of conjugate acid through titration methods is utilized to determine the total alkalinity.

2.4 Esterification

Esterification of used coconut cooking oil was processed in a three-neck flask set up with a cooling condenser and magnetic stirrer. The catalyst was dispersed into methanol, then stirred and added used cooking oil whose FFA content > 1%. This mixture was heated at 65 ℃ for 3 hours. Optimization was carried out by variations of catalyst weight (1, 3, and 5%), temperatures (45, 55, and 65 ℃), and mole ratios of oil:methanol (1:6, 1:9, 1:12, and 1:15). Then, the oil and catalyst were separated, and FFA levels were calculated. The oil with the lowest FFA level was used in the transesterification stage.

2.5 Transesterification

The Zr/CaO weighing 5% (w/w) was dispersed in methanol with 1:30 of oil:methanol mole ratio. The 20 g of esterified oil was added, then heated at 65 ℃ for 2 h. Catalyst and oil produced by the transesterification process were separated. Next, the solution was put in the separatory funnel then added saturated NaCl to separate the methyl ester, glycerol, and water. The formed methyl ester was added with Na_2SO_4 to bind and eliminate the water formed.

2.6 Product characterisation

Fourier Transform Infrared spectrophotometer (FT-IR, Shimadzu Prestige-21) is used to analyze functional groups of catalyst, then measured at 4000-400 cm^{-1} wavenumbers with KBr pellets. X-Ray Diffraction (XRD, PHILIPS XPert MPD) diffractometer with operational conditions set at 40 kV with nickel filter and Cu Kα (λ = 1.54 Å) at 2θ = 5-80° is utilized to characterize the crystallinity structures of catalysts. Scanning Electron Microscope (SEM, JEOL JSM-6510) adjusted with Energy Dispersive X-Ray (EDX, JED-2300 Analysis Station, 20kV) test, can be known surface morphology and elemental analysis of catalysts. Adsorption desorption methods at 77 K with the standard Brunauer-Emmett-Teller (BET) methods using a surface area analyzer (Nova-Quantachrome Instrument) result of surface area and pore distribution of the catalyst. Gas Chromatography and Mass Spectra using GC-MS instruments (Shimadzu QP2010S) give the biodiesel composition data formed. The magnitude of the used coconut cooking oil converted into methyl ester is known through the results of integration on ^{1}H-NMR (JEOL ECS-40) spectra and was calculated using the Knothe equation (Knothe, 2020).

$$C_{ME}=100\times\frac{5\times I_{ME}}{5\times I_{ME}+9\times I_{TG}} \qquad \textbf{Eqn. 1}$$

Where C_{ME} = methyl ester conversion, I_{ME} = methyl ester integration, I_{TG} = triglyceride integration.

3. Results and Discussion

3.1 Characterization of SO_4/ZrO_2 acid catalyst

In the present work, the observation of FTIR spectra of the pure ZrO_2, 0.5 M; 0.7 M; 0.9 M SO_4/ZrO_2 is presented in **Figure 1**. These spectra show band absorption at wavenumber 748-501 cm^{-1} presented a stretching vibration of Zr-O-Zr (Kuwahara *et al*., 2014). The absorption bands at 3449 and 1636 cm^{-1} indicate bending and stretching -OH water-coordinated vibrations onto the materials (Patel *et al*., 2013). Development of sulfate ions in zirconia material caused new uptake at wavenumbers 1226, 1157, 1080, and 1002 cm^{-1} showing S=O asymmetric vibration, S=O symmetric vibration, SO asymmetric vibrations, and SO symmetric vibrations (Sohn *et al*., 2003).

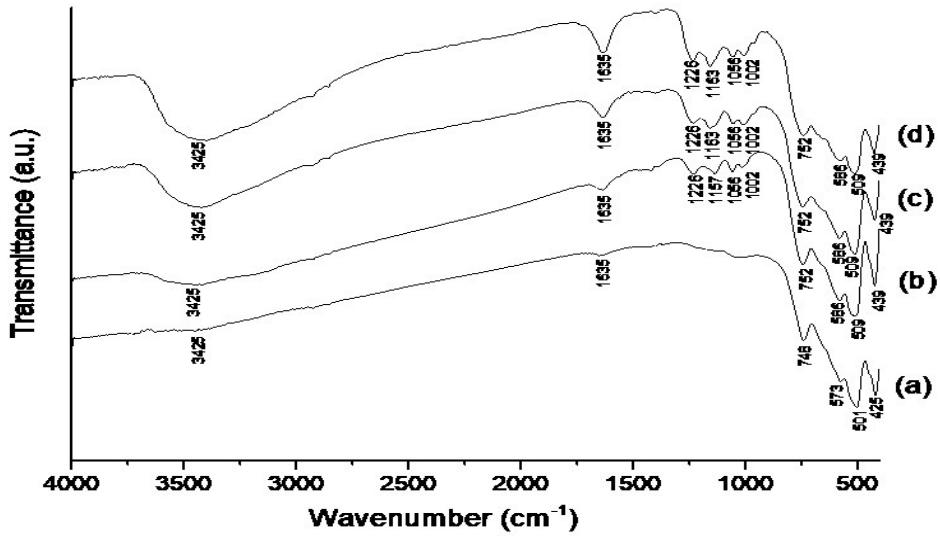

Figure 1. FT-IR spectra of (a) ZrO_2, (b) 0.5 M SO_4/ZrO_2, (c) 0.7 M SO_4/ZrO_2, (d) 0.9 M SO_4/ZrO_2

The four new absorption bands are characteristic bands whose presence of zirconium cation (Zr^{4+}) coordinated with inorganic chelate from bidentate sulfate ion. The intensity of sulfate ion uptake continued to increase with increasing concentration of sulfate ion, and the sharpest uptake shown in

0.9 M SO_4/ZrO_2 demonstrating the most dispersed sulfate ions in the catalyst. Acidity test results for ZrO_2 nanopowder; 0.5 M; 0.7 M; 0.9 M SO_4/ZrO_2 are 1.17; 1.20; 1.66; and 1.76 mmol NH_3 g^{-1}, respectively. The total acidity values continue to increase as the sulfate ion concentration increases due to the formation of Brønsted acid site from bridging on the Zr-OH group and Lewis acid site from Zr ion, whose a weak coordination bond with the acid site (Hauli *et al*., 2018). Related to **Figure 2**, an absorption that shows the presence of Brønsted acid site of NH_4^+ ions appeared at wavenumber 1404 cm^{-1}, whereas Lewis acid sites are presented at wavenumber 1118 cm^{-1} (Rey-Bueno *et al*., 1995). The intensity of ammonia absorptions for Brønsted and Lewis acid sites is getting higher along with increasing H_2SO_4 concentration.

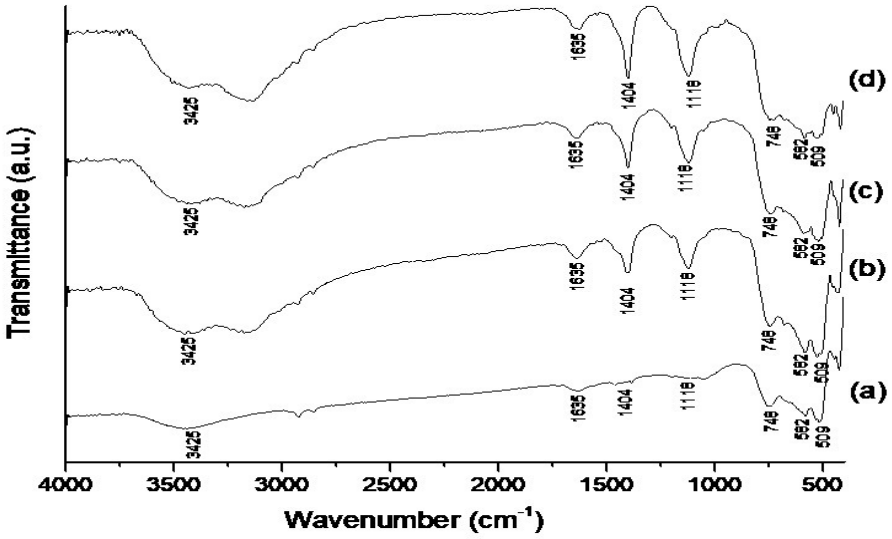

Figure 2. FT-IR spectra after acidity test of (a) ZrO_2, (b) 0.5 M SO_4/ZrO_2, (c) 0.7 M SO_4/ZrO_2, (d) 0.9 M SO_4/ZrO_2

The effect of calcination temperature of sulfate groups bound to the zirconia material showed in **Figure 3**. At 400 and 500 °C, four bands of sulfate group absorptions indicated that sulfate groups were well dispersed on zirconia. At 600 and 700 °C, the absorption intensity of the sulfate group at 1250-850 cm^{-1} decreased due to this higher calcination temperature since sulfate decomposes at a temperature above 500 °C (Tyagi *et al*., 2009).

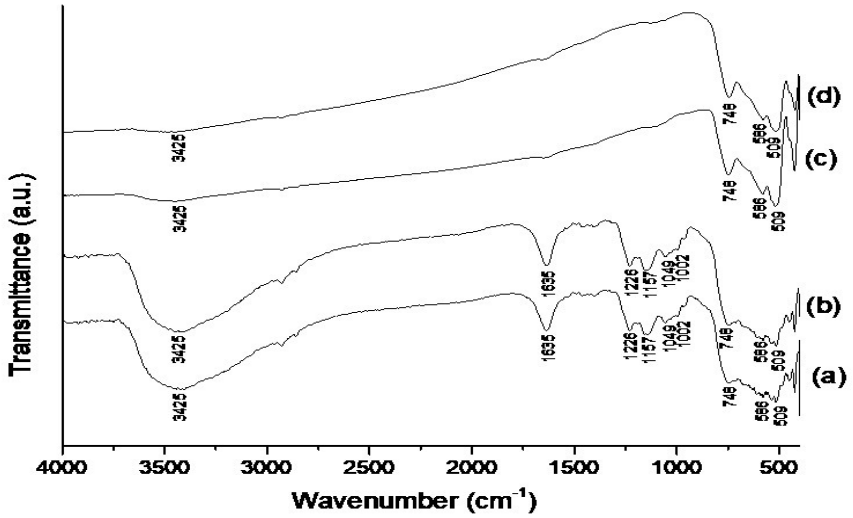

Figure 3. FT-IR spectra of (a) 0.9 M SO_4/ZrO_2-400, (b) 0.9 M SO_4/ZrO_2-500, (c) 0.9 M SO_4/ZrO_2-600, (d) 0.9 M SO_4/ZrO_2-700

Acidity test results for 0.9 M $SO_4/ZrO2$ -400, 0.9 M SO_4/ZrO_2-500, 0.9 M SO_4/ZrO_2-600, and 0.9 M SO_4/ZrO_2-700 were1.06; 1.98; 0.47; and 0.36 mmol NH_3 g^{-1}, respectively. The same patterns are also shown in **Figure 4** that the intensity of ammonia uptake increases at 400 and 500 °C then decreases at the temperature above 500 °C, indicating the sulfate groups that adsorbs ammonia were lost.

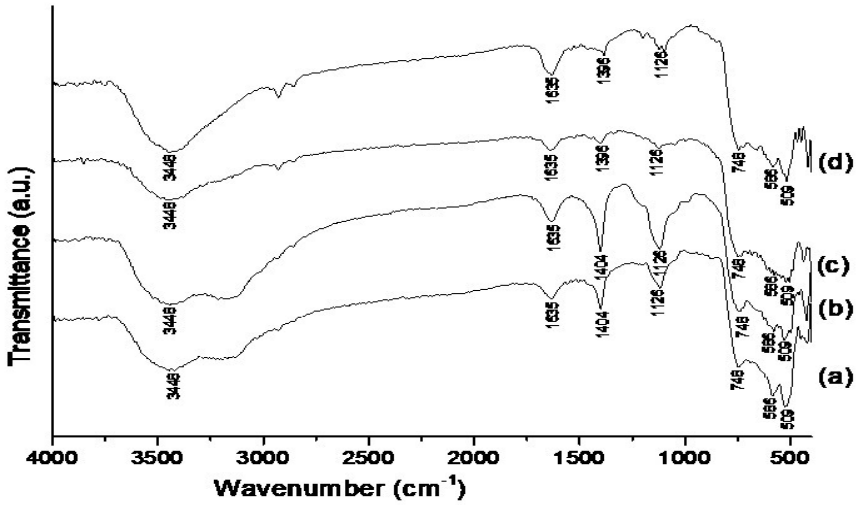

Figure 4. FT-IR spectra after acidity test of (a) 0.9 M SO_4/ZrO_2-400, (b) 0.9 M SO_4/ZrO_2-500, (c) 0.9 M SO_4/ZrO_2-600, (d) 0.9 M SO_4/ZrO_2-700

The XRD spectrum in **Figure 5** shows that ZrO_2 catalyst and SO_4/ZrO_2 catalyst at different calcination temperatures has a monoclinic and metastable tetragonal crystalline phase. According to previous research, ZrO_2 and 0.9 M SO_4/ZrO_2 have monoclinic crystalline phases confirmed through their high peaks at 2θ = 28.21° and 31.46° (Patel *et al*., 2013; Rachmat et al. 2017). The intensity of the monoclinic crystal phase increased with rising calcination temperature due to the loss of sulfate ions, which are loaded in zirconia nanopowder (Hauli *et al*., 2018). Zirconia has three crystalline phases, namely monoclinic (stable up to the temperature of 1140 °C), tetragonal (1140-2370 °C), and cubic (above 2370 °C). Fu et al. (2009) studied that the sulfate ion loaded on zirconia precursors and then calcined at the temperature 600 °C has a tetragonal crystalline phase (Fu *et al*., 2009). This study did not acquire the tetragonal crystalline phase because the raw material used came from commercial zirconia nanopowder. Both monoclinic and tetragonal crystalline phase has good catalytic activity.

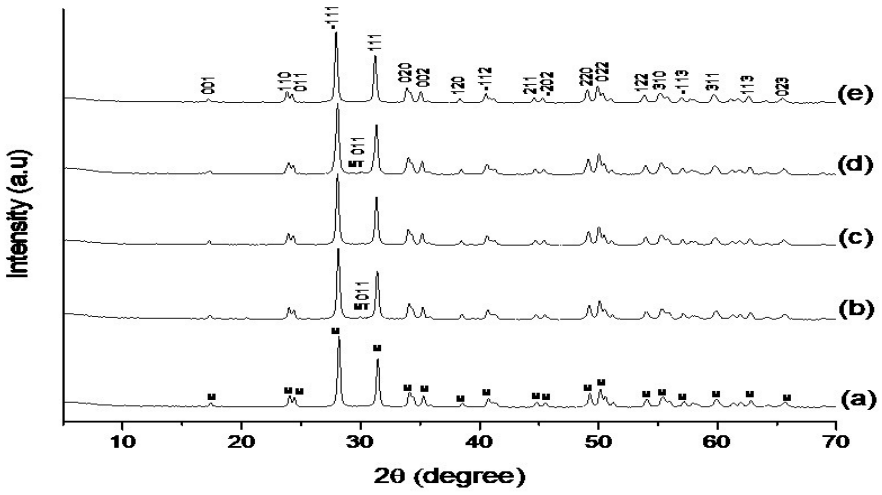

Figure 5. XRD diffractogram results of (a) ZrO_2, (b) 0.9 M SO_4/ZrO_2-400, (c) 0.9 M SO_4/ZrO_2-500, (d) 0.9 M SO_4/ZrO_2-600, (e) 0.9 M SO_4/ZrO_2-700

SEM results in **Figure 6** show no significant morphological changes in ZrO_2 and 0.9 M SO_4/ZrO_2-500, and both catalysts exhibit agglomeration. The presence of sulfate groups on zirconia is confirmed through EDX data which showed the presence of S atoms of 0.60% in **Table 1**.

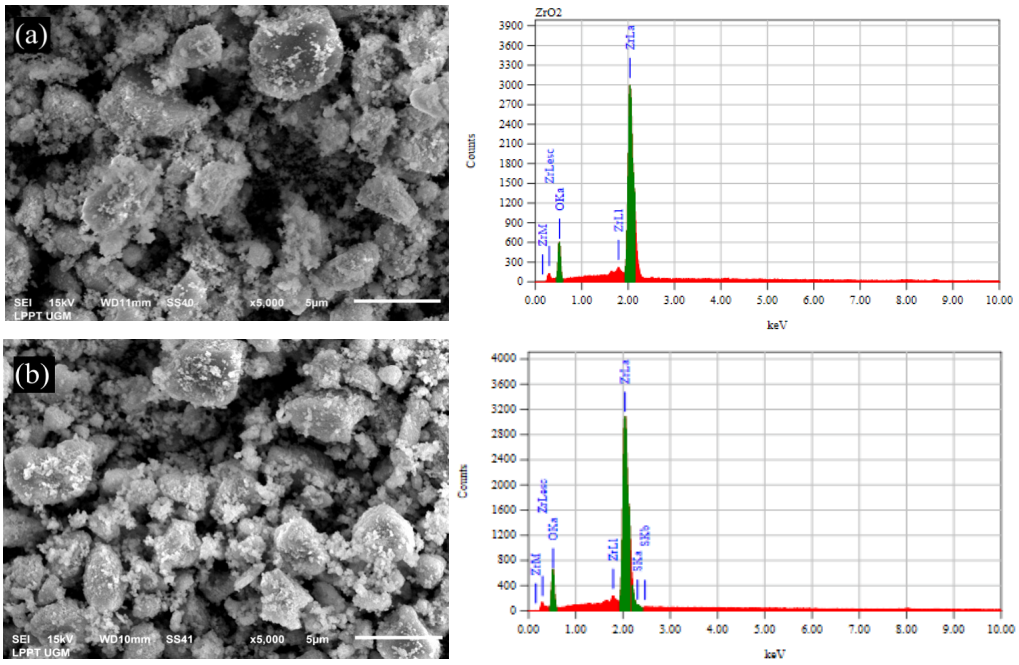

Figure 6. SEM and EDX results of (a) ZrO_2, and (b) 0.9 SO_4/ZrO_2-500 at 5000× magnification

Table 1. EDX results of ZrO_2 and 0.9 M SO_4/ZrO_2-500

Catalyst	Element Mass (%)		
	Zr	O	S
ZrO_2	74.03	25.97	-
0.9 M SO_4/ZrO_2-500	72.92	26.48	0.60

Based on **Table 2**, ZrO_2 has a larger surface area than 0.9 M SO_4/ZrO_2-500. The decrease in surface area on zirconia impregnated with sulfate ion occurred due to employing strong acid causes damage to some bonds leading to shrinkage of the skeleton. The same phenomenon was shown in the pore diameter of the catalyst that decreased due to impregnation. The SO_4/ZrO_2-500 had a pore diameter of 20.99 nm, and it is able to adsorb triglyceride molecules measuring at 2.5 nm in esterification or transesterification reactions.

Table 2. Surface area analysis results of ZrO_2 and 0.9 M SO_4/ZrO_2-500

Catalyst	Specific surface area ($m^2\ g^{-1}$)	Total pore volume ($cm^3\ g^{-1}$)	Average pore diameter (nm)
ZrO_2	5.89	3.305×10^{-2}	22.43
SO_4/ZrO_2-500	5.35	2.807×10^{-2}	20.99

3.2 Characterization of Zr/CaO base catalyst

The spectra FT-IR of Zr/CaO with various weight percentage of Zr is presented in **Figure 7**. These spectra show that the wavenumber of 3641 cm^{-1} has a sharp absorption band representing the hydroxyl group in CaO. Absorption bands that indicate asymmetric stretch, out-of-plane bent, and in-plane bent for CO_3^{2-} ion molecules showed at 1471, 877, and 684 cm^{-1} (Lesabani *et al.*, 2013). The Zr^{4+} cation was

successfully impregnated on CaO material characterized by the appearance of absorption in the wavenumber area of 748-501 cm^{-1} that indicates the vibration of Zr-O and Zr-O-Zr. The alkalinity test results of pure CaO; 1%; 3%; 5% Zr/CaO catalysts calcined at 700 °C are 20.62; 24.62; 23.99; and 15.15 mmol g^{-1}, respectively. In this study, the Zr^{4+} cation was derived from acidic $ZrOCl_2.8H_2O$ to reduce alkalinity value along with the increase in the number of precursors used.

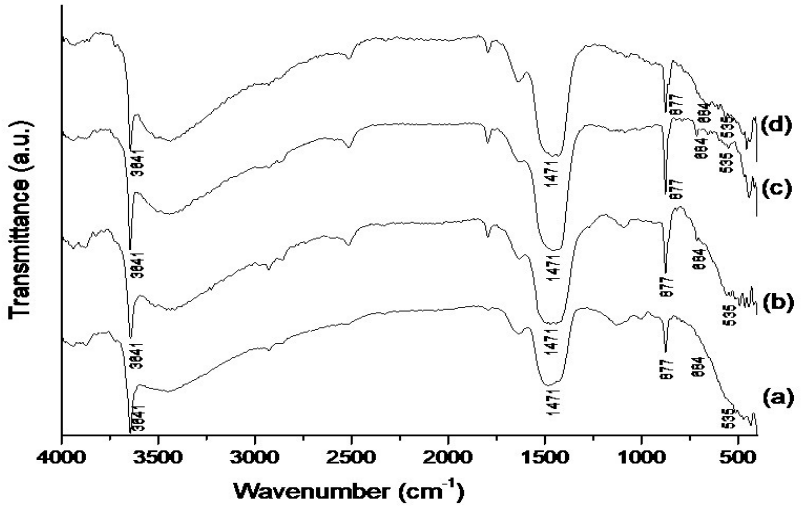

Figure 7. FT-IR spectra of (a) CaO, (b) 1% Zr/CaO, (c) 3% Zr/CaO, (c) 5% Zr/CaO calcinated at 700 °C

The catalyst with the highest total alkalinity, 1% Zr/CaO, was calcined at 600, 700, 800, and 900 °C then tested for its alkalinity values, which shown in **Figure 8**. The 1% Zr/CaO at all of the various calcination temperatures have Zr^{4+} cations characterized by absorptions in the area of 748-501 cm^{-1}. This data shows that the addition of calcination temperature causes a shortening of absorption intensity. The alkalinity test results of 1% Zr/CaO calcined at 600, 700, 800, and 900 °C are 20.62; 24.62; 26.94; and 27.78 mmol g^{-1}, respectively. The catalyst 1% Zr/CaO alkalinity values increase along with the increase of temperature due to the thermal decomposition of these catalysts.

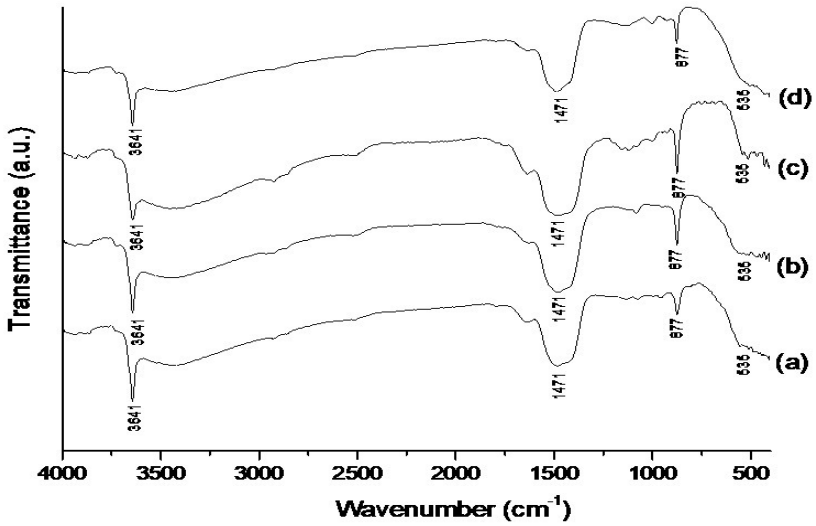

Figure 8. FT-IR spectra of (a) 1% Zr/CaO-600, (b) 1% Zr/CaO-700, (c) 1% Zr/CaO-800, (d) 1% Zr/CaO-900

The structure and crystallinity of the catalyst were established by XRD analysis. The catalyst with the highest total alkalinity values is calcined with a temperature variation of 600-900 °C, as shown in

Figure 9. In the CaO diffractogram, portlandite-$Ca(OH)_2$ (hexagonal) crystalline phase is shown at 2θ = 28.73; 29.44; 34.14; 47.03; and 50.87° (JCPDS 044-1481). In the area of 2θ = 31.65° appears a small intensity peak describing the appearance of the crystalline phase of $CaZrO_3$, which has been influenced with Zr^{4+} ion loaded on the surface zirconia (Kaur *et al*., 2014). On the other hand, there is a peak at 2θ = 54.28° indicates the presence of lime-CaO (cubic) (Xia *et al*., 2014). The peak of calcite-$CaCO_3$ (rhombohedral) appears at 2θ = 29.44° (JCPDS 001-0837), and the intensity of this peak diminishes with the increment of calcination temperature. Calcination temperature increases cause thermal decomposition, which impacts the decline in the intensity of $Ca(OH)_2$ and $CaCO_3$ along with their conversion into CaO. On the other hand, the thermal decomposition is able to increase the alkalinity of the catalyst since the alkalinity of technical CaO was greater than $Ca(OH)_2$ and much greater than $CaCO_3$ (Dehkordi *et al*., 2012). Literature show that Nickel, Iron, Cobalt, Copper… nanoparticles subjected to thermal decomposition at low temperature of 400 °C in an open atmosphere (Barakat *et al*., 2013; Unni *et al*., 2017; Zheng *et al.* 2016; Abdel-Monem *et al.* 2017)

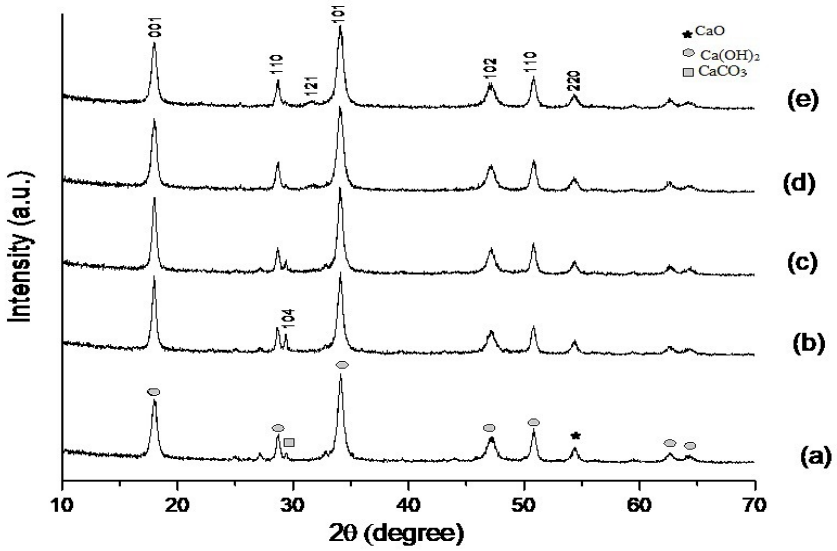

Figure 9. XRD Diffractogram of (a) CaO, (b) 1% Zr/CaO-600, (c) 1% Zr/CaO-700, (d) 1% Zr/CaO-800, (e) 1% Zr/CaO-900

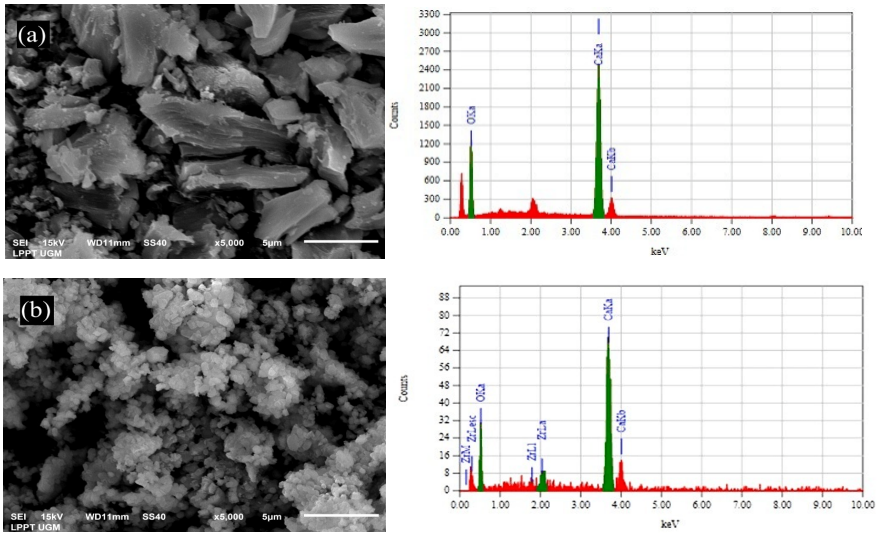

Figure 10. (a) SEM and EDX results of (a) CaO, and (b) 1% Zr/CaO-900 at 5000x magnification

SEM data of CaO and 1% Zr/CaO-900 catalysts show significant differences. CaO has an irregular morphology because it has a gap that is then used to impregnate the Zr^{4+} cation. Modification of CaO with Zr^{4+} cations calcined at 900 °C causes damage to CaO indicated by smaller structure size, as shown in **Figure 10**. The successful impregnation of Zr^{4+} cations onto CaO can be confirmed through EDX results shown in **Table 3**, which displays the presence of Zr elements of 7.17%.

Table 3. EDX results of CaO and 1% Zr/CaO-900

Catalyst	Element Mass (%)		
	Ca	O	Zr
CaO	71.47	28.53	-
1% Zr/CaO-900	64.54	28.28	7.17

The size of CaO and 1% Zr/CaO-900 surface area are presented in **Table 4**. This data indicates that Zr^{4+} impregnation on the 1% Zr/CaO-900 catalyst formed a smaller surface area than pure CaO. The Zr^{4+} ions were substituted into the Ca^{2+} cation caused a decline in the specific surface area of the catalyst. The Zr/CaO catalysts calcined at high temperatures affected the loss of the $CaCO_3$ crystalline phase, which was confirmed through the XRD as well. $CaCO_3$ crystalline loss causes added basicity to the catalyst, so it has good catalytic activity (Lesbani *et al*., 2013). The surface area decreases on the 1% Zr/CaO-900 as the result of CaO structure being damaged and exfoliated. Furthermore, calcination at high temperatures causes thermal decomposition, which could reduce the surface area of CaO. This data is similar to a study by Kaur and Ali (2014) that present 15% Zr/CaO calcined at 700 °C results in a specific surface area of 1.86 $m^2\ g^{-1}$ yet still have a good catalytic activity because the alkalinity value of the catalyst more effects it compared to its specific surface area (Kaur and Ali, 2014). These results followed several kinds of literature reporting that high alkalinity results in good catalytic activity in transesterification reactions (Lesbani *et al*., 2013; Dehkordi *et al*., 2012; Singh *et al*., 2008).

Table 4. Surface area analysis results of CaO and 1% Zr/CaO-900

Catalyst	Specific surface area ($m^2\ g^{-1}$)	Total pore volume ($cm^3\ g^{-1}$)	Average pore diameter (nm)
CaO	122.4	2.409×10^{-1}	7.872
1% Zr/CaO-900	14.53	3.182×10^{-2}	8.762

3.3 Preparation of used cooking oil

The production of biodiesel begins with the preparation of used coconut cooking oil for the esterification stage, followed by the transesterification to form fatty acid methyl ester (FAME) using methanol as a reactant. The preparation involved purifying the oil to remove impurities and then heated to omit the water content in used coconut cooking oil. The obtained saponification value of used coconut cooking oil is 213.88 mg KOH g^{-1} and has a molecular weight of 787.40 g/mol and an FFA content of 1.18%. The conversion of this used coconut oil into methyl ester formed moisture content of more than 0.3% and FFA more than 0.5%, and it caused a saponification reaction that will deactivate the catalyst involved. Hence, initial treatment through esterification reaction was needed to reduce FFA levels in oil.

3.3 Esterification

The esterification reaction was achieved with three various treatments, i.e. catalyst weight, oil:methanol mole ratio, and reaction temperature. The graph of catalyst weight influence at decreased

FFA levels in **Figure 11** shows that catalyst with 5% weight has the largest decrease in FFA levels of 43.13%. The decrease in FFA levels of used cooking oil intensifies with the increase in weight of the catalyst, indicating that the more catalysts used in the esterification stage, the more active sites quantities, which play an important role in their catalytic activity (Fadhil, 2013).

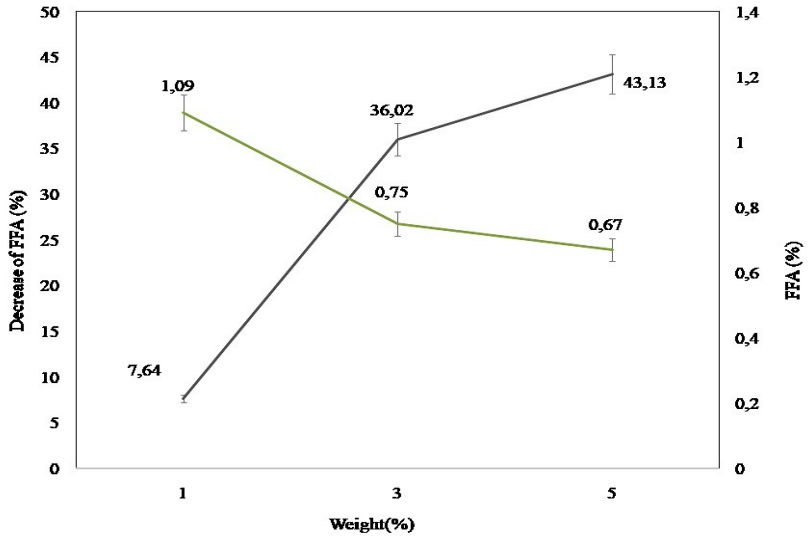

Figure 11. Graph of the relationship between catalyst weight percentage and coconut oil FFA level at 1:9 of oil:methanol mole ratio and 65 °C reaction temperature under 3 h duration

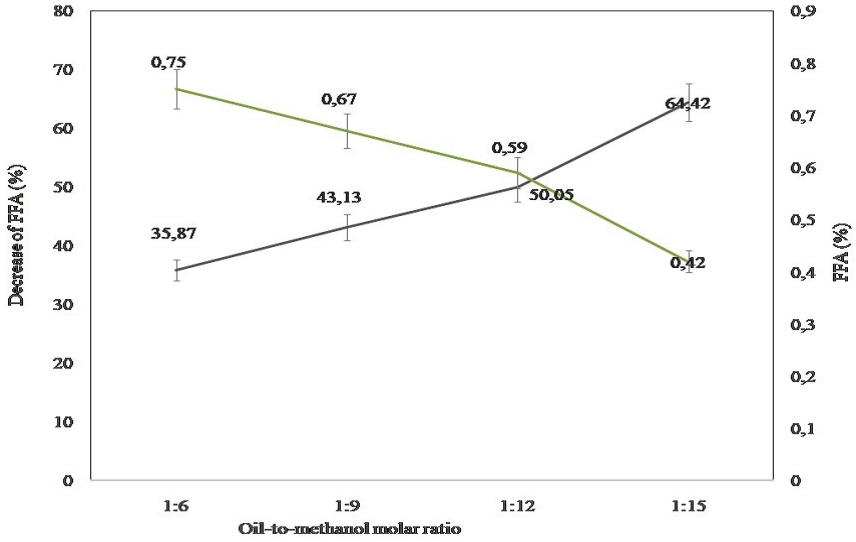

Figure 12. Graph of the relationship between oil:methanol mole ratio and coconut oil FFA levels for 5% catalyst weight and 65 °C reaction temperature under 3 hours duration

Esterification is a reversible reaction, and the treatment of excessive amounts of methanol can transfer the equilibrium towards product formation (Zarrag *et al*., 2013). The effect of oil:methanol mole ratio is presented in **Figure 12** with a ratio range of 1:9-1:15. FFA levels of used cooking oil were reduced by 35.87% at 1:6 of oil:methanol mole ratio and continued to increase with the increasing mole ratio of oil:methanol. In this study, the lowest FFA content resulted from oil esterified with 1:15 oil:methanol mole ratio of 0.42%, attaining a decrease in FFA levels of 64.42%. This data indicates that the greater the oil:methanol mole ratio used the reaction, the more equilibrium will be shifted towards larger product formation. Oil:methanol mol ratio used is comparable to the resulting methoxy ions. At a low ratio of methanol, the fraction of oil in the mixture is high, and most catalysts are in the

oil fraction. Oil covered the catalyst surface that caused the formation of methoxy ions will decrease (La Ore *et al*., 2020).

Reaction temperature plays a crucial role in the triglyceride esterification reaction. The optimum temperature for the esterification reaction ranges from the boiling point of alcohol (Saravanan *et al*., 2012). In this study, methanol was used because it is low-cost and can react rapidly with vegetable oil. The effect of reaction temperature can be observed in **Figure 13** which shows the greatest decrease in FFA levels (64.42%) was obtained with the rise of reaction temperature (65 °C) that is similar to the boiling point of methanol (65 °C) under atmospheric pressure (Pati *et al*., 2009). This optimal reaction temperature shortens the reaction time and increases the reaction rate as a result of the decreased oil viscosity. Methanolysis reaction carried out with reaction temperature over the boiling point of methanol causes evaporation, resulting in reduced contact of oil and catalyst and decreased methyl ester formation (Dehkordi *et al*., 2012; Fadhil, 2013).

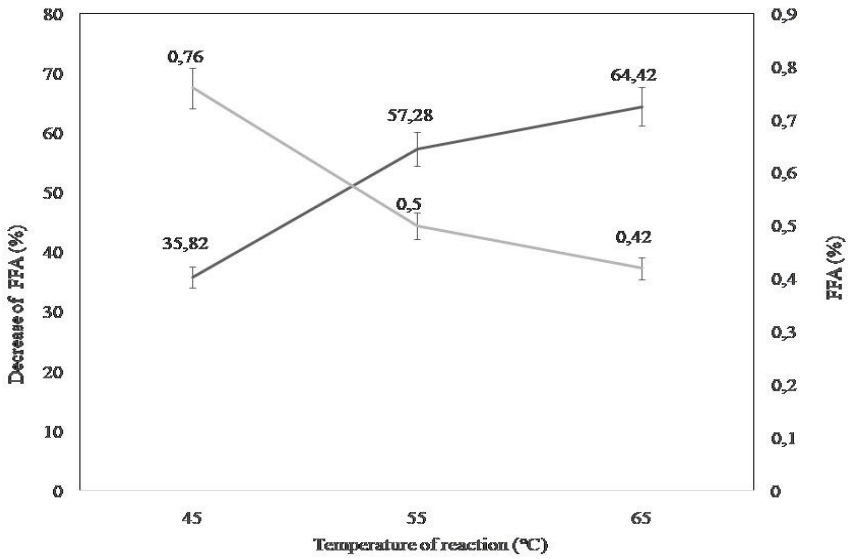

Figure 13. Graph of the relationship between reaction temperatures and coconut oil FFA contents at 5% catalyst weight, 1:15 of oil:methanol mole ratio under 3 hours duration

3.3 Transesterification

The used cooking oil lost through the esterification process was executed in the transesterification stage to be converted into biodiesel. The transesterification reaction was committed under 5% catalyst weight conditions: 1:30 of oil:methanol mole ratio, 65 °C reaction temperature for 2 hours. The use of methanol as a reactant compared to other alcohols was because methanol had a short chain that results in induction effects and a large electron-donating ability meaning that its reactivity was large. Stoichiometrically, methyl ester was obtained by reacting one mole of triglyceride with three moles of methanol in the transesterification reaction. Excess methanol aims to shift towards methyl ester formation and eliminate product molecules from the catalyst surface to recreate the active site (Kaur and Ali, 2014).

FTIR spectra in **Figure 14** can be used to detect the formation of biodiesel, through functional groups characteristic of methyl ester. The FTIR spectra of esterification and transesterification products showed absorptions at wavenumbers 2855 and 2924 cm^{-1}, indicating asymmetric and symmetric vibrations of CH_3 group in –CO–O–CH_3. The remaining bands at 1458 cm^{-1}, 1373-1111 cm^{-1}, and 725 cm^{-1} result from alkane bonds (–CH), stretching vibration (-CO) of the ester group, and –CH_2 group absorption, respectively (Dehkordi *et al*., 2012). The presence of glycerol seen at wavenumber 1744

cm^{-1} and $–CH_2$ at wavenumber 1373 cm^{-1} was indicated by the absorption of the carbonyl group (Rabelo *et al*., 2015). The characteristics spectra of biodiesel presented in the FT-IR spectra of transesterification show new absorption stretching vibration for $–O-CH_3$ at wavenumber 1196 cm^{-1} and $–O-CH_2-C$ vibration absorption band at 1018 cm^{-1}.

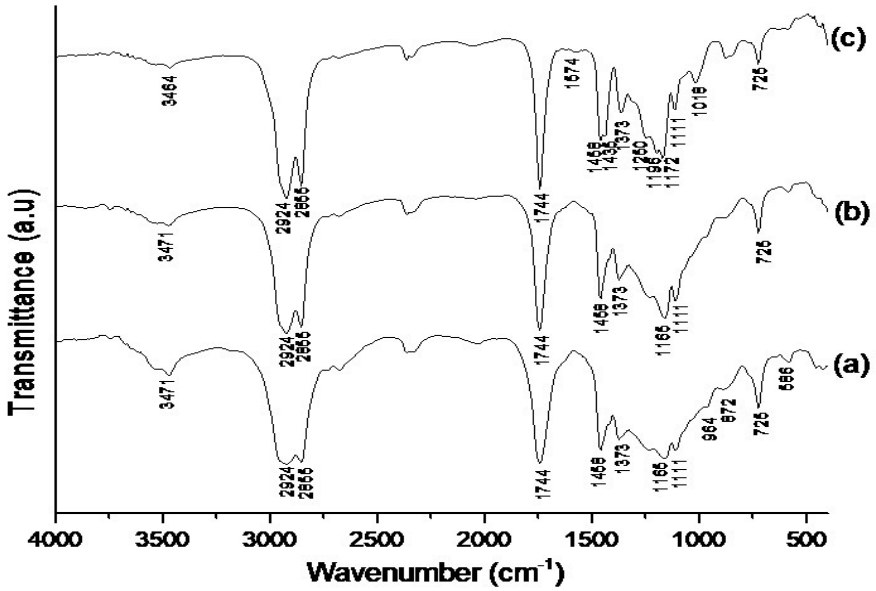

Figure 14. FT-IR spectra of (a) used coconut cooking oil, (b) esterified oil, and (c) transesterified oil

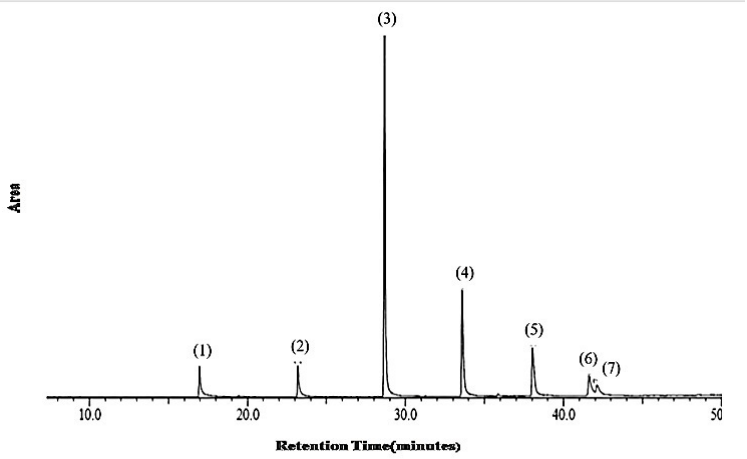

Figure 15. Chromatogram of transesterified oil

Gas chromatography analysis of transesterified oil in **Figure 15** shows the formation of seven peaks representing the formed methyl ester compositions with the highest peak at number 3. **Table 5** shows the composition of methyl esters in biodiesel consisting of methyl laurate (50.48%), methyl myristate (19.05%), methyl stearate (11.05%), methyl 11-octadecanoic (6.09%), methyl octanoate (5.25%), methyl decanoate (5.05), and methyl octadecanoate (3.03%). The highest peak comes from methyl laurate with 50.48% surface area, and the second-highest is methyl myristate with 19.05%. This data is also supported by several works (Soudagar *et al*., 2020; Kumar *et al*., 2010; Oliveira *et al.*, 2010) that obtained products in the form of methyl laurate and methyl myristate from the transesterification of coconut oil as the raw material. Laore et al. (2020) also obtained 49.10% methyl laurate and 18,06% methyl myristate from the conversion of low-grade crude palm oil into biodiesel production (La Ore *et al*., 2020).

Table 5. Retention time and area of chromatogram peak of GC-MS results

Peak	Compound	Molecular weight (g mol^{-1})	Retention time (minutes)	Surface area (%)
1	Methyl octanoate	158	16.96	5.25
2	Methyl decanoate	186	23.19	5.05
3	Methyl laurate	214	28.67	50.48
4	Methyl myristate	242	33.58	19.05
5	Methyl stearate	298	38.03	11.05
6	Methyl 11-octadecanoate	296	41.61	6.09
7	Methyl octadecenoate	298	42.11	3.03

The ^{1}H-NMR spectra in **Figure 16** show chemical shifts at 4.1-4.3 ppm and 5.2 ppm, specific to protons in triglycerides from used coconut cooking oil with integration values 1 and 0.55. In transesterified oil, all triglycerides have been converted into methyl esters can be seen at a peak loss in the 4.1-4.3 ppm chemical shift. In addition, there is a new peak at 3.5 ppm, with an integration value of 3 representing the methoxy group in methyl esters. Quantitative analysis to determine the scale of methyl ester formed was obtained by substituting the value of proton integration of triglycerides with protons in the methoxy group in **Eqn. 1**. Based on the Knothe equation, the conversion of used coconut cooking oil succeeded transform into methyl ester is 62.5%.

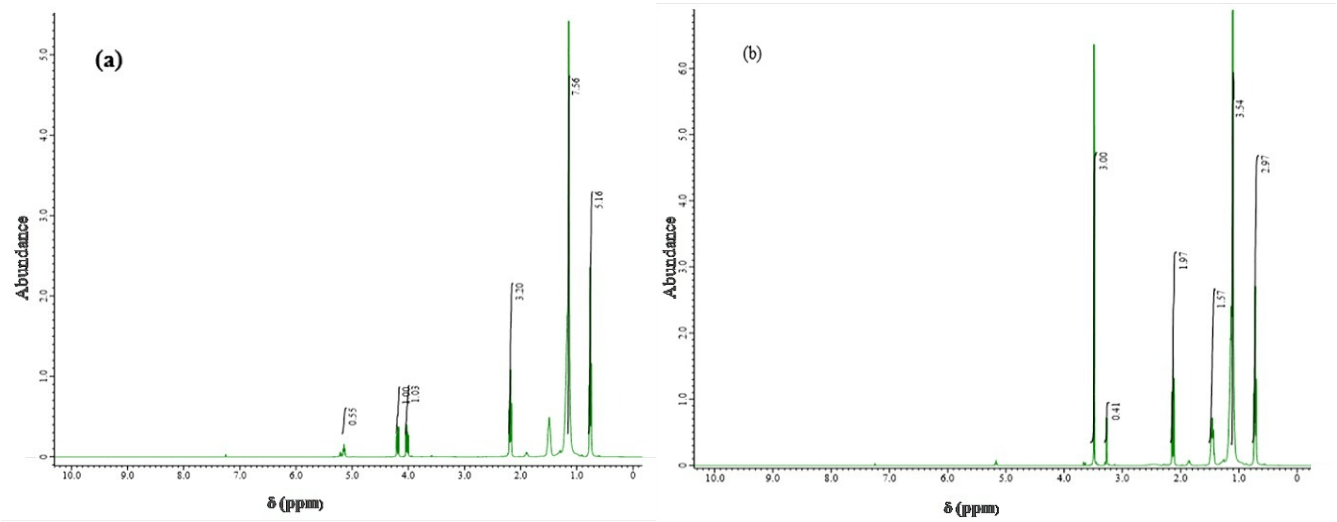

Figure 16. Chromatogram of transesterified

Conclusion

The SO_4/ZrO_2 acid catalyst was successfully synthesized in various H_2SO_4 concentrations and temperature reactions. The optimum condition of this synthesis process was reached by employing 0.9 M H_2SO_4 and 500 °C of temperature reaction. The highest total acidity of 1.98 mmol g^{-1} was obtained by 0.9 M SO_4/ZrO_2-500 acid catalyst and succeeded in reducing the FFA oil from 1.18% to 0.42% in the esterification reaction. However, the best total alkalinity was achieved by the 1% Zr/CaO-900 base catalyst, which generated 27.78 mmol g^{-1}. The esterification product was then transesterified under the optimum condition, 1% Zr/CaO-900 base catalysts with 5% catalyst weight, 1:30 of oil:methanol mole ratio, 65 °C reaction temperature, and 2 h of duration time in the synthesis process. Remarkably, this catalyst has capable of converting to methyl ester of 62,5%, mostly methyl laurate compound.

Acknowledgement: This research was carried out thanks to a funding from PTUPT DRPM-DIKTI (Project No. 2737/UN1.DITLIT/DIT-LIT/LT/2019). The authors would like to thank the Indonesian Ministry of Research, Technology, and Higher Education for their financial support.

Disclosure statement: *Conflict of Interest:* The authors declare that there are no conflicts of interest.

Compliance with Ethical Standards: This article does not contain any studies involving human or animal subjects.

References

Abdel-Monem Y.K., Emam S.M., Okda H.M.Y. (2017) Solid state thermal decomposition synthesis of CuO nanoparticles from coordinated pyrazolopyridine as novel precursors, *Journal of Materials Science: Materials in Electronics* 28(3), 2923-2934

Aman D., El-Hafiz D. R. A., Ebiad M. A. (2018) Thermodynamic parameter for steam reforming reaction of biodiesel by-product using nano-sized perovskite catalysts, *Mor. J. Chem.,* 6(3), 466–479

Banković-Ilić I. B., Miladinović M. R., Stamenković O. S., Veljković V. B., (2017) Application of nano CaO–based catalysts in biodiesel synthesis. *Renew. Sustain. Energy Rev.* 72, 746–760. https://doi.org/10.1016/j.rser.2017.01.076

Barakat A., Suleiman M., Aldwayyan A.S., Hammouti B., Ben Hadda T., Al-Noaimi M., Haddad S.F., Boshaala A., Warad I. (2013) One Step Synthesis of NiO Nanoparticles via Solid-State Thermal Decomposition at Low-Temperature of Novel Aqua(2,9-dimethyl-1,10-phenanthroline)NiCl2 Complex, Int. J. Mol. Sci. 14, 23941-23954

Cao F., Chen Y., Zhai F., Li J., Wang J., Wang X., Wang S., Zhu W., (2008) Biodiesel production from high acid value waste frying oil catalyzed by superacid heteropolyacid. *Biotechnol. Bioeng.,* 101, 93–100. https://doi.org/10.1002/bit.21879

Clearfield A., Serrette G. P. D., Khazi-Syed A. H., (1994) Nature of hydrous zirconia and sulfated hydrous zirconia. *Catal. Today*, 20, 295–312. https://doi.org/10.1016/0920-5861(94)80008-1

Dehkordi A. M., Ghasemi M., (2012) Transesterification of waste cooking oil to biodiesel using Ca and Zr mixed oxides as heterogeneous base catalysts. *Fuel Process Technol*., 97, 45–51. https://doi.org/10.1016/j.fuproc.2012.01.010

Delarmelina M., Deshmukh G., Goguet A., Catlow C.R.A., Manyar H. (2021) Role of Sulfation of Zirconia Catalysts in Vapor Phase Ketonization of Acetic Acid. *J Phys Chem C Nanomater Interfaces.* 125(50), 27578-27595. doi: 10.1021/acs.jpcc

Fadhil A. B., (2013) Biodiesel production from beef tallow using alkali-catalyzed transesterification. *Arab J. Sci. Eng.,* 38, 41–47. https://doi.org/10.1007/s13369-012-0418-8

Fu B., Gao L., Niu L., Wei R., and Xiao G., (2009) Biodiesel from waste cooking oil via heterogeneous superacid catalyst SO_4^{2-}/ZrO_2. *Energy and Fuels,* 23, 569-572. https://doi.org/10.1021/ef800751z

Garba A. A., Usman B. (2021) Optimization and evaluation of biodiesel quality produced from cattle fat using CaO/Al_2O_3 as catalyst, *Mor J. Chem.* 9, 132-141

Hauli L., Wijaya K., Armunanto R., (2018) Preparation and characterization of sulfated zirconia from a commercial zirconia nanopowder. *Orient. J. Chem.*, 34, 1559–1564. doi.org/10.13005/ojc/340348

Hsiao M. C., Kuo J. Y., Hsieh S. A., Hsieh P. H., Hou S. S., (2020) Optimized conversion of waste cooking oil to biodiesel using modified calcium oxide as catalyst via a microwave heating system. *Fuel*. https://doi.org/10.1016/j.fuel.2020.117114

Kaur N., Ali A., (2013) Lithium ions-supported magnesium oxide as nano-sized solid catalyst for biodiesel preparation from mutton fat. *Energy sources part A recover Util Environ. Eff.,* 35, 184–192. https://doi.org/10.1080/15567036.2011.592912

Kaur N., Ali A., (2014) Kinetics and reusability of Zr/CaO as heterogeneous catalyst for the ethanolysis and methanolysis of Jatropha crucas oil. *Fuel Process Technol*., 119, 173–184. https://doi.org/10.1016/j.fuproc.2013.11.002

Knothe G., (2000) Monitoring a progressing transesterification reaction by fiber-optic near infrared spectroscopy

with correlation to 1H nuclear magnetic resonance spectroscopy. *J. A. Oil Chem. Soc.,* 77, 489–493. https://doi.org/10.1007/s11746-000-0078-5

Kumar D., Ali A. (2012) Nanocrystalline K-CaO for the transesterification of a variety of feedstocks: Structure, kinetics and catalytic properties. *Biomass and Bioenergy*, 46, 59–468. https://doi.org/10.1016/j.biombioe.2012.06.040

Kumar G., Kumar D., Singh S., Kothari S., Bhatt S., Singh, C. P. (2010) Continuous low cost transesterification process for the production of coconut biodiesel. *Energies,* 3, 43–56. doi.org/10.3390/en3010043

Kuwahara Y., Fujitani T., Yamashita H., (2014) Esterification of levulinic acid with ethanol over sulfated mesoporouszirconosilicates: Influences of the preparation conditions on thestructural properties and catalytic performances. *Catal. Today*, 237, 18–28. https://doi.org/10.1016/j.cattod.2013.11.008

La Ore M. S., Wijaya K., Trisunaryanti W., Saputri W. D., Heraldy E., Yuwana N. W., Hariani P. L., Budiman A., Sudiono S., (2020) The synthesis of SO_4/ZrO_2 and Zr/CaO catalysts via hydrothermal treatment and their application for conversion of low-grade coconut oil into biodiesel. *J. Environ. Chem. Eng.*, https://doi.org/10.1016/j.jece.2020.104205

Lesbani A., Tamba P., Mohadi R., Fahmariyanti, (2013) Preparation of calcium oxide from Achatina fulica as catalyst for production of biodiesel from waste cooking oil. *Indones. J. Chem*. 13, 176–180. doi: 10.22146/ijc.21302

Ma F., Hanna M. A. (1999) Biodiesel production: a review1Journal Series #12109, agricultural research division, institute of agriculture and natural resources, university of nebraska–lincoln.1. *Bioresour. Techno*., 70, 1–15. https://doi.org/10.1016/S0960-8524(99)00025-5

Mabate M. P., Maqunga N. P., Ntshibongo S., Maumela M., Bingwa N. (2023) Metal oxides and their roles in heterogeneous catalysis: special emphasis on synthesis protocols, intrinsic properties, and their infuence in transfer hydrogenation reactions, *SN Applied Sciences* 5, 196, https://doi.org/10.1007/s42452-023-05416-6

Mahardika I. B. P., Trisunaryanti W., Triyono T., Wijaya D. P., Dewi K. (2017) Transesterification of used cooking oil using CaO/MCM-41 catalyst synthesized from lapindo mud by sonochemical method. *Indones. J. Chem.* 17, 509–515. https://doi.org/10.22146/ijc.26561

Mathiyazhagan M., Ganapathi A., (2011) Factors affecting biodiesel production. *Research in Plant Biology*, 1, 1–5

Niyas M. M., Shaija A. (2023) Biodiesel production from coconut waste cooking oil using novel solar powered rotating flask oscillatory flow reactor and its utilization in diesel engine, *Thermal Science and Engineering Progress,* 40, 101794, ISSN 2451-9049, https://doi.org/10.1016/j.tsep.2023.101794

Nurhayati, Anita S., Amri T. A., Linggawati A., (2017) Esterification of crude palm oil using H_2SO_4 and transesterification using CaO catalyst derived from Anadara granosa. *Indones. J. Chem*., 17, 309–315. https://doi.org/10.22146/ijc.24909

Oliveira J. F. G., Izabelly Larissa Lucena I. L., Saboya R. M. A., Rodrigues M. L., Torres A. E. B., Fernandes F. A. N., Cavalcante C. L., Parente E. J. S., (2010) Biodiesel production from waste coconut oil by esterification with ethanol: The effect of water removal by adsorption. *Renew. Energy*, 35, 2581–2584. https://doi.org/10.1016/j.renene.2010.03.035

Patel A., Brahmkhatri A., Singh N. (2013) Biodiesel production by esterification of free fatty acid over sulfated zirconia. *Renew. Energy*, 51, 227–233. https://doi.org/10.1016/j.renene.2012.09.040

Patil P. D., Deng S., (2009) Transesterification of camelina sativa oil using heterogeneous metal oxide catalysts. *Energy and Fuels,* 23, 4619–4624. https://doi.org/10.1021/ef900362y

Rabelo S.N., Ferraz V. P., Oliveira L. S., Franca A. S., (2015) FTIR analysis for quantification of fatty acid methyl esters in biodiesel produced by microwave-assisted transesterification. *Int. J. Environ. Sci. Dev.* 6, 964–969. doi: 10.7763/IJESD.2015.V6.730

Rachmat A., Trisunaryanti W., Sutarno, Wijaya K., (2017) Synthesis and characterization of sulfated zirconia mesopore and its application on lauric acid esterification. *Mater. Renew. Sustain. Energy*, https://doi.org/10.1007/s40243-017-0097-1

Rey-Bueno F D., García-Rodríguez A., Mata-Arjona A., Rey-Pérez-Caballero F.J.D. (1995) Acidity of montmorillonite-(Ce OR Zr) phosphate cross-linked compounds. doi.org/10.1346/CCMN.1995.0430505

Rozina, Ahmad M., Elnaggar A. Y., Teong L. K., Sultana S., Zafar M., Munir M., Hussein E. E., Ul Abidin S. Z. (2022) Sustainable and eco-friendly synthesis of biodiesel from novel and non-edible seed oil of Monotheca buxifolia using green nano-catalyst of calcium oxide, *Energy Conversion and Management: X,* 13, 2022, 100142, ISSN 2590-1745, https://doi.org/10.1016/j.ecmx.2021.100142

Saravanan K., Tyagi B., Bajaj H. C., (2012) Esterification of caprylic acid with alcohol over nano-crystalline sulfated zirconia. *J. Sol-Gel Sci. Technol*., 62, 13–17. https://doi.org/10.1007/s10971-011-2671-9

Sekewael S.J.; Pratika R.A.; Hauli L.; Amin A.K.; Utami M.; Wijaya K. (2022) Recent Progress on Sulfated Nanozirconia as a Solid Acid Catalyst in the Hydrocracking Reaction. *Catalysts* 12, 191. https://doi.org/10.3390/catal12020191

Singh A. K., Fernando S. D., (2008) Transesterification of soybean oil using heterogeneous catalysts. *Energy and Fuels*, 22, 2067–2069. https://doi.org/10.1021/ef800072z

Sohn J. R., Seo D. H., (2003) Preparation of new solid superacid catalyst, zirconium sulfate supported on γ-alumina and activity for acid catalysis. https://doi.org/10.1016/j.cattod.2003.09.010

Soudagar M. E. M., Afzal A., Kareemullah M., (2020) Waste coconut oil methyl ester with and without additives as an alternative fuel in diesel engine at two different injection pressures. *Energy sources, part A Recover. Util. Environ. Eff*., https://doi.org/10.1080/15567036.2020.1769775

Suprapto, Fauziah T. R., Sangi M. S., Oetami T. P., Qoniah I., Prasetyoko D., (2016) Calcium oxide from limestone as solid base catalyst in transesterification of Reutealis trisperma oil. *Indones. J. Chem*., 16, 208–213. https://doi.org/10.22146/ijc.21165

Tyagi B., Mishra M. K., Jasra R. V., (2009) Solvent free synthesis of 7-isopropyl-1,1-dimethyltetralin by the rearrangement of longifolene using nano-crystalline sulfated zirconia catalyst. *J. Mol. Catal. A Chem.*, 301, 67–78. https://doi.org/10.1016/j.molcata.2008.11.011

Xia S., Guo X., Mao D., Shi Z., Wu G., Lu G. (2014) Biodiesel synthesis over the CaO-ZrO_2 solid base catalyst prepared by a urea-nitrate combustion method. *RSC Adv*., 4, 51688–51695. https://doi.org/10.1039/C4RA11362D

Unni M., Uhl A. M., Savliwala S., Savitzky B. H., Dhavalikar R., Garraud N., Arnold D. P., Kourkoutis L. F., Andrew J. S., and Rinaldi C. (2017) Thermal Decomposition Synthesis of Iron Oxide Nanoparticles with Diminished Magnetic Dead Layer by Controlled Addition of Oxygen, *ACS Nano*, 11, 2, 2284–2303, https://doi.org/10.1021/acsnano.7b00609

Usman B. & Dambazau M. A. (2018) Optimisation of Base Catalysed Transesterification of Fish Oil for Biodiesel Production Using Response Surface Methodology, *Mor. J. Chem.* 6 N°2 (2018) 318-327

Wang Q., Wenlei Xie W., Guo L. (2022), Molybdenum and zirconium oxides supported on KIT-6 silica: A recyclable composite catalyst for one–pot biodiesel production from simulated low-quality oils, *Renewable Energy,* 187, 907-922, ISSN 0960-1481, https://doi.org/10.1016/j.renene.2022.01.122

Yamaguchi T., (1994) Application of ZrO_2 as a catalyst and a catalyst support. *Catal. Today*, 20, 199–217. https://doi.org/10.1016/0920-5861(94)80003-0

Zarrag A., May E., Medhat I., (2013) On the Spectroscopic Analyses of Protein. *J. Comput. Theor. Nanosci*., 10, 2375–2379. https://doi.org/10.1166/jctn.2013.3217

Zein Y. M., Anal A. K., Prasetyoko D., Qoniah I., (2016) Biodiesel production from waste palm oil catalyzed by hierarchical ZSM-5 supported calcium oxide. *Indones. J. Chem.*, 16, 98–104. https://doi.org/10.22146/ijc.21184

Zheng Y-C., Li Z-Q., Xu J., et al. (2016) Cobalt Oxide @ Carbonized Wings Composite: Preparation and Catalytic Performance for Decomposition of Ammonium Perchlorate[J]. *Chinese Journal of Energetic Materials*, 24(3), 256-260